



Article

# Effect of Stress Ratio and Loading Inclination on the Fatigue Life of Carbon-Fiber-Reinforced Polymer Composites: Multiscale Analysis Approach

Rajeev Kumar<sup>1</sup>, Sunny Zafar<sup>1</sup>, Himanshu Pathak<sup>1</sup> , Murugan Subramani<sup>2</sup> , Chuan Li<sup>3</sup> and Song-Jeng Huang<sup>2,\*</sup>

- <sup>1</sup> Composite Design and Manufacturing Research Group, School of Mechanical and Materials Engineering, Indian Institute of Technology Mandi, Mandi 175075, Himachal Pradesh, India; d19043@students.iitmandi.ac.in (R.K.); sunnyzafar@iitmandi.ac.in (S.Z.); himanshu@iitmandi.ac.in (H.P.)
- <sup>2</sup> Department of Mechanical Engineering, National Taiwan University of Science and Technology, No. 43, Section 4, Keelung Rd, Da'an District, Taipei 106335, Taiwan; smurugan2594@gmail.com
- <sup>3</sup> Department of Biomedical Engineering, National Yang Ming Chiao Tung University, Hsinchu 112304, Taiwan; cli10@nycu.edu.tw
- \* Correspondence: sgjghuang@mail.ntust.edu.tw; Tel.: +886-2-2737-6485

**Abstract:** The integration of mesoscale modeling and macroscale experimentation has emerged as a promising approach for understanding and predicting the mechanical behavior and fatigue performance of fiber-reinforced polymer composites. In this work, the mean field homogenization technique is implemented to predict the fatigue performance of the carbon-fiber-reinforced polymer composites under cyclic loading conditions. To predict the number of fatigue cycles, Modified Gerber criteria are used with the stress-based Tsai–Hill failure indicator. Fatigue strength factor ( $\alpha$ ) and creep rupture strength factor ( $\beta$ ) are experimentally evaluated and further implemented in a computational approach to predict fatigue life cycles of the composite. The effect of composite constituents, stress ratio, and loading direction are investigated in detail against the fatigue performance of the composite. Fatigue cycles are predicted at individual matrix and fiber levels at various stress ratios of 0.2, 0.4, 0.6, and 0.8 at different loading inclinations. The experimental results are compared with the mesoscale S–N curves.

**Keywords:** carbon-fiber-reinforced polymer composites; fatigue cycles; mean field homogenization; stress ratio; S–N curve



**Citation:** Kumar, R.; Zafar, S.; Pathak, H.; Subramani, M.; Li, C.; Huang, S.-J. Effect of Stress Ratio and Loading Inclination on the Fatigue Life of Carbon-Fiber-Reinforced Polymer Composites: Multiscale Analysis Approach. *J. Compos. Sci.* **2023**, *7*, 406. <https://doi.org/10.3390/jcs7100406>

Academic Editors: Michela Simoncini and Archimede Forcellese

Received: 9 August 2023  
Revised: 8 September 2023  
Accepted: 22 September 2023  
Published: 24 September 2023



**Copyright:** © 2023 by the authors. Licensee MDPI, Basel, Switzerland. This article is an open access article distributed under the terms and conditions of the Creative Commons Attribution (CC BY) license (<https://creativecommons.org/licenses/by/4.0/>).

## 1. Introduction

Composite materials are significant in various fields due to their unique properties and numerous advantages over traditional materials. Composite materials are known for their exceptional strength-to-weight ratio [1]. They offer high strength and stiffness while being significantly lighter than traditional materials like metals. This property is crucial in aerospace, automotive, and sporting goods industries, where weight reduction is vital for performance, fuel efficiency, and cost savings [2,3]. Fiber composites are often used in applications subjected to cyclic loading or repeated stresses, such as aircraft wings, wind turbine blades, and automotive components. Fatigue failure can occur when the material experiences repetitive loading below the ultimate strength, leading to progressive damage accumulation and eventual failure. Understanding and mitigating fatigue failure is crucial for ensuring composite structures' long-term performance and reliability [4]. Fatigue failure can significantly reduce fiber composite structure durability and service life. It can result in a loss of structural integrity, compromising the safety and functionality of the components. By considering fatigue-failure mechanisms and designing composite structures to withstand cyclic loading, engineers can enhance their durability, extend their service life, and reduce the risk of catastrophic failures. Fiber-reinforced polymer (FRP)

composites exhibit various fatigue-failure mechanisms due to the complex interaction between fibers, matrix, and interfaces [5]. These mechanisms can lead to progressive damage accumulation and the eventual failure of the composite material. Some of the key fatigue-failure mechanisms in FRP composites are matrix cracking, debonding, fiber–matrix interface damage, fiber–matrix shear, and fiber failure [6,7]. Understanding and characterizing these fatigue-failure mechanisms is essential for accurately predicting the fatigue life and designing fatigue-resistant FRP composite structures. Various experimental techniques, computational models, and multiscale approaches are employed to study these mechanisms and develop effective strategies for improving the fatigue performance of FRP composites. Mesoscale fatigue analysis of fiber composites focuses on understanding the behavior of the material at an intermediate-length scale between the micro scale and the macro scale. Mesoscale fatigue analysis provides valuable insights into the damage mechanisms and failure modes that occur within the composite material [8]. Homogenization techniques are frequently used at the meso scale to determine the effective properties of materials with complex microstructures [9–11]. Homogenization refers to the process of determining the effective or averaged properties of the composite as a whole, based on the properties of its constituent materials and their spatial arrangement. Composite materials are typically composed of two or more distinct phases, such as fibers embedded in a matrix, and homogenization aims to provide a simplified representation of their behavior at a macroscopic level. Various mathematical and numerical techniques are employed for homogenization. These techniques can range from simple methods like the rule of mixtures (linear combination of properties based on volume fractions) to more complex methods like finite-element analysis (FEA) applied to representative volume elements (RVEs) [12–14].

Mesoscale fatigue analysis is often integrated into multiscale modeling approaches to capture the interaction between different-length scales. By linking mesoscale models with macroscale structural analysis, the effects of mesoscale damage mechanisms on the overall structural response can be assessed. This integration can provide a more comprehensive understanding of fatigue behavior, enabling more accurate predictions of fatigue life and structural integrity. Carbon-fiber composites are known for their high strength-to-weight ratio and are commonly used in various applications where lightweight and high-performance materials are required, such as the aerospace, automotive, and sporting goods industries [15]. However, like any other material, carbon-fiber composites are susceptible to fatigue failure when subject to cyclic loading. Mesoscale fatigue behavior in carbon-fiber composites is influenced by several factors, including composite architecture, fiber orientation, resin matrix properties, interfacial bonding, and manufacturing defects. At the mesoscale level, fatigue-damage mechanisms such as fiber–matrix debonding, fiber breakage, matrix cracking, and delamination between layers can occur. To characterize and predict the mesoscale fatigue behavior of carbon-fiber composites, researchers have used various experimental and computational techniques. These techniques include cyclic loading tests on representative composite specimens, non-destructive evaluation methods such as ultrasonic inspection, and numerical modeling using finite-element analysis (FEA) or multiscale modeling approaches [16,17]. Mesoscale fatigue of carbon-fiber composites refers to the fatigue behavior of these materials at the intermediate-length scale between the microscopic and macroscopic levels. It involves understanding the mechanisms and properties of carbon-fiber composites under cyclic loading conditions, which can lead to structural failure over time. Carbon-fiber composites are composed of carbon fibers embedded in a matrix material, typically polymer resin. The orientation and arrangement of these fibers play a crucial role in determining the composite's mechanical properties and fatigue behavior. The high strength and stiffness of carbon fibers combined with the lightweight matrix result in excellent overall mechanical performance. However, cyclic loading can initiate and propagate fatigue cracks at the mesoscale level, leading to reduced strength and ultimately the failure of the composite structure. Several factors influence mesoscale fatigue behavior in carbon-fiber composites. The composite architecture, including fiber volume fraction, fiber orientation, and arrangement, affects the material's

load-transfer mechanisms and stress distribution. The properties of the matrix material, such as its stiffness, toughness, and resistance to fatigue crack growth, also impact the composite's fatigue behavior. The interfacial bonding between the fibers and the matrix is critical for load transfer and preventing fiber–matrix debonding. During cyclic loading, various fatigue-damage mechanisms can occur at the mesoscale level. These mechanisms include fiber–matrix debonding, fiber breakage, matrix cracking, and delamination between layers [6]. Fiber–matrix debonding refers to the separation of the fibers from the matrix, which reduces load-transfer efficiency and leads to local stress concentrations. Fiber breakage occurs when the applied cyclic load exceeds the strength of individual fibers, resulting in a loss of load-carrying capacity. Matrix cracking refers to the formation of cracks within the matrix material due to cyclic loading, which can propagate and lead to significant damage. Delamination occurs when there is separation between adjacent layers of the composite, often at the interfaces, causing a reduction in overall structural integrity.

Brunbauer et al. developed a fatigue-life prediction method for carbon-fiber laminates using a finite-element solver. The predicted cyclic life was correlated with the experimental study and it was found that the software underestimated the experimental data [18]. Zhang et al. presented a meso model for the fatigue damage of fiber-reinforced composites, where the effect of stress ratio and off-axis fatigue behavior is considered. The results showed that the proposed fatigue model can accurately describe the fatigue life of unidirectional composite laminates [19]. Shokrieh et al. developed an energy method based on the fatigue model for a unidirectional polymer composite with constant amplitude tension–tension fatigue loading. Experimental data were used to verify the model, and results showed a good agreement with the fatigue model. The model is capable of predicting the fatigue life of unidirectional fiber composites at a positive stress ratio and various fiber orientation angles [20]. Huang et al. investigated the fatigue behavior of filament-wound carbon-fiber-reinforced composites with different lay-ups. The results showed that the stress ratio significantly affects the composites' failure mechanism. An empirical model was developed that integrated the effect of stress ratio in the fatigue-damage parameter to find the fatigue life of the CFRP composites [21]. Xu et al. used the finite-element approach at the meso level for tension–tension fatigue of unidirectional composites. The matrix-dominated and fiber-dominated fatigue was separately considered. In the model fiber rupture, matrix crack was used as fatigue-failure criteria of the fiber-reinforced composites. The model was capable of estimating the tension–tension fatigue life of different composites [22]. To characterize and predict the mesoscale fatigue behavior of carbon-fiber composites, researchers employed a combination of experimental and computational techniques. Experimental tests, such as cyclic loading tests on representative composite specimens, provide valuable data on fatigue life, damage evolution, and failure modes. Computational models, such as finite-element analysis (FEA) or multiscale modeling approaches, simulate the stress distribution and damage progression within the composite, helping to understand the underlying mechanisms and predict fatigue life. By studying mesoscale fatigue behavior, researchers aim to understand the fundamental mechanisms that contribute to fatigue-damage accumulation in carbon-fiber composites. This knowledge aids in the development of more accurate predictive models, designing more durable composite structures, and optimizing manufacturing processes to enhance the fatigue resistance of carbon-fiber composites. It allows engineers to assess the long-term performance and reliability of composite components, ensuring their safe operation under cyclic loading conditions.

In the literature, it can be understood that mesoscale modeling is crucial to understanding the fatigue behavior of the composites. Ensuring a robust and well-integrated meso–macro structure helps enhance the durability and reliability of composites. This is particularly important in applications where the composite material is subjected to cyclic loading. In addition, meso–macro integration is much less explored in the literature, which could be crucial in obtaining accurate fatigue results for fiber-reinforced composites and helps engineers optimize the design and performance of carbon-fiber composite structures in realistic applications, ensuring their safety and reliability. Meso–macro integration is

an ongoing area of research and development in composites. Continued advancements in the understanding and control of mesoscale properties can lead to innovative composite materials with novel properties and applications. The following are the specific objectives of the manuscript:

- A robust and efficient multiscale (meso–macro) computational approach has been developed and implemented for fatigue performance prediction of carbon-fiber-reinforced polymer composite. The effect of composite constituents, stress ratio, and loading direction are investigated in detail against the fatigue performance of the composite.
- Fatigue strength factor ( $\alpha$ ) and creep rupture strength factor ( $\beta$ ) are experimentally evaluated and further implemented in a computational approach to predict fatigue-life cycles of a composite.
- Interaction between fibers and matrix at the meso scale is analyzed against the damage initiation under cyclic loading conditions. S–N curves are obtained at stress ratios of 0.2, 0.4, 0.6, and 0.8 with loading inclination of 15°, 30°, 45°, and 60°.

## 2. Materials and Methods

The polyacrylonitrile-based long carbon-fiber PC402H was used as the reinforcing material. High-modulus (~240 GPa) carbon fibers were procured from Bhor Chemicals and Plastics Pvt. Ltd., Mumbai, India. Epichlorohydrin bisphenol-A epoxy resin with amine hardener was used as the matrix material and mixed in a ratio of 100:60.

The CFRPCs were manufactured using a vacuum-assisted resin infusion microwave curing process (VARIMC). The process is known for the manufacture of high-grade fiber composites with minimum defects [23,24]. Microwaves help in curing the composites uniformly with a high degree of cure, and vacuum (0.1 MPa) ensures high density by removing the entrapped air from the composites [25]. The composites were manufactured with carbon-fiber weight percentages of 45%, 55%, and 65%. The polytetrafluoroethylene (PTFE) mold and vacuum bagging material used was microwave transparent. Aluminum tape was used to avoid arcing in the microwave by proper masking of carbon fibers. A multimode commercial microwave applicator (Make: VB Ceramics, Chennai; Model: 700DEG) with constant microwave power of 360 W and fixed microwave frequency of 2.45 GHz was used. The temperature was monitored by an IR pyrometer mounted on the microwave applicator. Other details of the manufacturing of the CFRPCs are mentioned in Table 1.

**Table 1.** Properties of the CFRPCs at various fiber mass fractions.

Properties	Fiber Mass Fraction		
	65%	55%	45%
Tensile Modulus (GPa)	92 ± 4.6	76 ± 3.1	54 ± 2.2
Axial Tensile Strength (MPa)	368 ± 13.8	306 ± 12.6	227 ± 9.2
In-Plane Tensile Strength (MPa)	44 ± 1.6	43 ± 1.2	41 ± 1.3
Shear Strength (MPa)	18 ± 0.6	16 ± 0.4	12 ± 0.4
Percentage Elongation	1.6 ± 0.05	2.0 ± 0.09	2.6 ± 0.11

The flow chart in Figure 1 illustrates the interaction between macro and meso scales in the investigation of fatigue behavior in carbon-fiber-reinforced polymer composites (CFRPCs). At the macro scale, experimental fatigue tests were conducted on CFRPCs with varying fiber mass fractions to gather data on their fatigue performance. The Goodman equation presents a linear relationship. If the exponent, denoted as “n”, takes a value of two, and the mean stress is normalized by the ultimate tensile strength, the equation transforms into the Gerber equation, which takes on a parabolic form. The Goodman equation has demonstrated remarkable effectiveness in addressing the impact of mean

stress within the tension–tension quadrant. The Goodman equation is widely utilized to determine the fatigue design limit of metals when subject to tensile mean stress at various fatigue-life durations. Nevertheless, it is worth noting that certain investigations have indicated that the actual influence of mean stress lies somewhere between the predictions of the Goodman equation and the Gerber equation. In the Modified Gerber equation, the mean stress is normalized using the creep rupture strength instead of the static tensile strength and can proficiently present the mean stress effect during the cyclic loading [26,27]. Subsequently, Modified Gerber equation parameters, a common fatigue model for ductile materials, were determined based on the experimental results. These experimentally determined parameters, along with the composite properties, were then fed to the Digimat® 2022.4 software, a multiscale modeling tool that can simulate the mechanical behavior of composites. By utilizing the Modified Gerber criteria and the Tsai–Hill failure indicator, the software predicted fatigue cycles under different loading directions and stress ratios. Finite-element (FE) simulations were conducted to further analyze the composite’s behavior and obtain von Mises stress contours at various loading conditions. Finally, the predicted S–N (stress–number of cycles) curves were compared and validated against the experimental fatigue data to assess the models’ and simulations’ accuracy and reliability. This comprehensive approach helps researchers and engineers gain insight into the fatigue performance of CFRPCs under different conditions and optimize their design and usage in various practical applications.

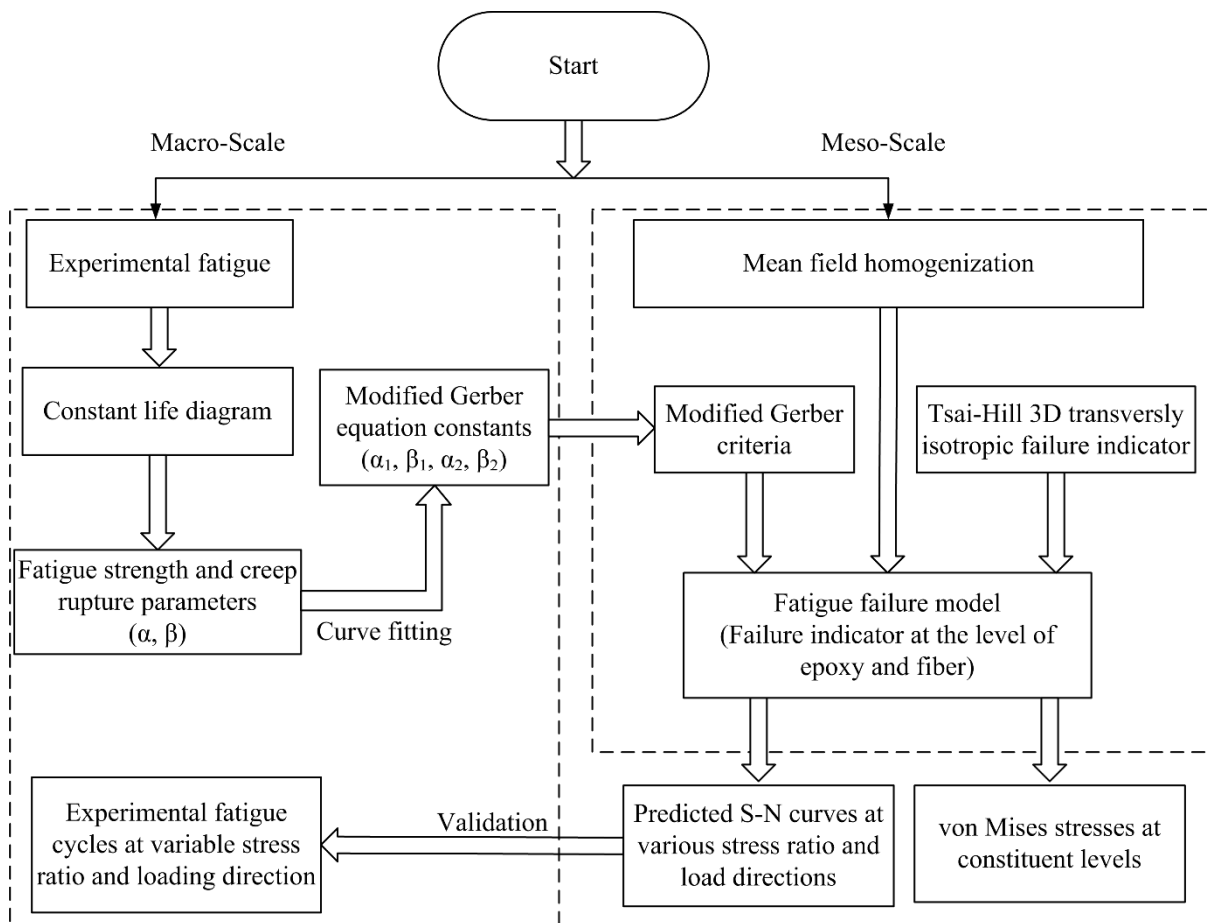


Figure 1. Flow chart for multiscale fatigue modeling.

## 2.1. Multiscale Fatigue Performance

### 2.1.1. Macro Scale

Tension–tension fatigue tests were conducted on an Instron 8802 hydraulic universal testing rig with an accuracy of  $\pm 0.2$  kN. At least five samples with the same parameters were used for the fatigue test to ensure repeatability. The tension–tension fatigue behavior was analyzed in accordance with ASTM 3479 [28]. The strength of the composites decreases rapidly after relatively few cycles but remains approximately constant up to around 80% of fatigue life [29]. Therefore, 0.8 of the original strength is taken as the fatigue life. The load was first increased to reach the maximum stress, and subsequently, constant amplitude load was applied for an infinite number of cycles or until the failure of the composite. The ultimate tensile strength (UTS) of the CFRPCs was calculated, and its different percentage levels were used to plot the maximum stress (S) versus number of cycles (N) to failure (S–N) curve for tension–tension fatigue analysis. The experiments were carried out with a symmetric triangular waveform with a stress ratio (R) of 0, 0.2, 0.4, and 0.6 at a fixed frequency of 10 Hz. All the experiments were carried out at a controlled room temperature ( $22 \pm 1$  °C). Emry cloth was used as the interface between grips and the specimen in the serrated wedge grips to avoid the sudden fracture at the gripping portion of the composites according to the ASTM standard D3039 [30]. At least three tensile–tensile fatigue experiments were conducted at each stress ratio and at three different stress amplitudes. A total of 36 fatigue experiments were initially conducted to draw the constant life diagram, which was further used to find the fatigue parameters. Finally, experimental S–N curves were drawn at different stress ratios and loading inclinations, and were compared with the predicted fatigue life.

The fracture mechanisms of CFRPCs under cyclic loading were analyzed using scanning electron microscopy (SEM) (Make: FEI, USA, Model: NOVA, NANO SEM). Gold coating of 5 nm was placed on the surface of specimens to avoid the formation of an electrostatic charge cloud.

### 2.1.2. Macroscale Modeling

Carbon-fiber composites exhibit complex microstructures, where the individual fibers interact with the surrounding matrix at the meso scale, and these interactions collectively influence the overall mechanical behavior of the material at the macro scale. Mesoscale modeling is implemented to know the effect of fatigue loading on the individual constituent of the composite. The mean field homogenization technique is utilized to find the mesoscale S–N curves at constituent levels. Mean field homogenization provides a computationally efficient way to estimate the effective properties of complex materials with microstructural heterogeneities [31].

The Representative Volume Element (RVE) approach is employed to capture the mesoscale behavior of the composite. RVE models consider the unit cell structure containing fibers and matrix, allowing for the analysis of stress and strain distributions within the composite under cyclic loading. Mallick and Zhou [27] proposed a modified version of the well-known stress-based Gerber criteria, which considers the influence of mean stress on the fatigue strength of glass fiber-reinforced polyamide-66 composites. The non-dimensional equation for the Gerber equation was derived by expressing it in terms of ultimate tensile strength and incorporating fatigue strength factors ( $\alpha$ ) and creep rupture strength factor ( $\beta$ ), as shown in Equation (1).

$$\frac{\sigma_a}{\alpha\sigma_u} + \left(\frac{\sigma_m}{\beta\sigma_u}\right)^2 = 1 \quad (1)$$

In the given equation, the parameters  $\alpha$  and  $\beta$  are to be adjusted, while  $\sigma_m$  represents the mean stress, and  $\sigma_a$  and  $\sigma_u$  represent the stress amplitude and ultimate tensile strength, respectively. Normalizing the data by  $\sigma_u$  enables the unification of the data considering sample orientation and atmospheric conditions.

The parameters  $\alpha$  and  $\beta$  are optimized to better fit the full database and take the power-law form, as shown in Equations (2a) and (2b).

$$\alpha = \alpha_1 N_c^{\alpha_2} \tag{2a}$$

$$\beta = \beta_1 N_c^{\beta_2} \tag{2b}$$

Here,  $N_c$  is the number of fatigue cycles and  $\alpha_1, \alpha_2, \beta_1,$  and  $\beta_2$  are the constants to be determined by curve fitting.

The Modified Tsai–Hill criterion, proposed by Bernasconi et al. [32] and De Monte et al. [33], incorporates the Tsai–Hill criterion adapted for cyclic loading to predict fatigue failure and considers the influence of fiber orientation relative to the loading direction. The stress-based Tsai–Hill failure indicator was used in conjunction with Modified Gerber fatigue criteria. The criterion incorporates both normal and shear stresses to evaluate material failure. It is commonly used to predict failure modes such as fiber rupture, matrix cracking, or delamination in fiber-reinforced composites. The Tsai–Hill equation, which corresponds to Axis 1, is given by Equation (3).

$$f_A = \sqrt{F_A(\sigma)} \text{ With}$$

$$F_A(\sigma) = \frac{\sigma_{11}^2}{X^2} - \frac{\sigma_{11}(\sigma_{22} + \sigma_{33})}{X^2} + \frac{\sigma_{22}^2 + \sigma_{33}^2}{Y^2} + \left(\frac{1}{X^2} - \frac{1}{Y^2}\right)\sigma_{22}\sigma_{33} + \frac{\sigma_{12}^2 + \sigma_{13}^2}{S^2} + \left(\frac{4}{Y^2} - \frac{1}{X^2}\right)X_{23}^2 \tag{3}$$

where  $\sigma_{ij}$  denotes the component of the stress amplitude corresponding to the local axis system, and X, Y, and S denote the axial, in-plane, and shear stress amplitude at failure.

The Tsai–Hill criterion is an empirical failure criterion that predicts failure based on a linear combination of the material’s strength properties. The Tsai–Hill criterion compares the composite’s stress components to their respective strength values and calculates a failure index. Failure is predicted if the failure index exceeds a predefined threshold (usually set to 1).

The various loading directions of 15°, 30°, 45°, and 60° to the fiber axis were used for the fatigue analysis of the CFRPCs, as shown in Figure 2.

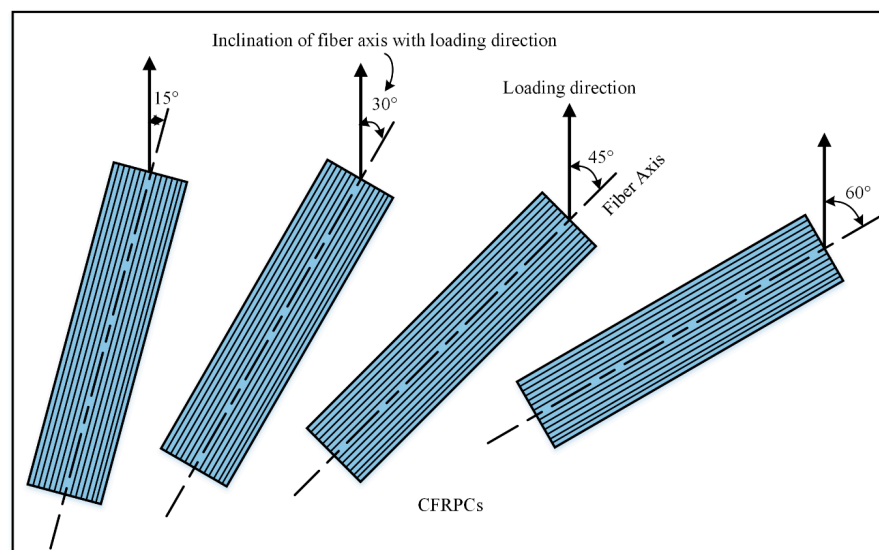
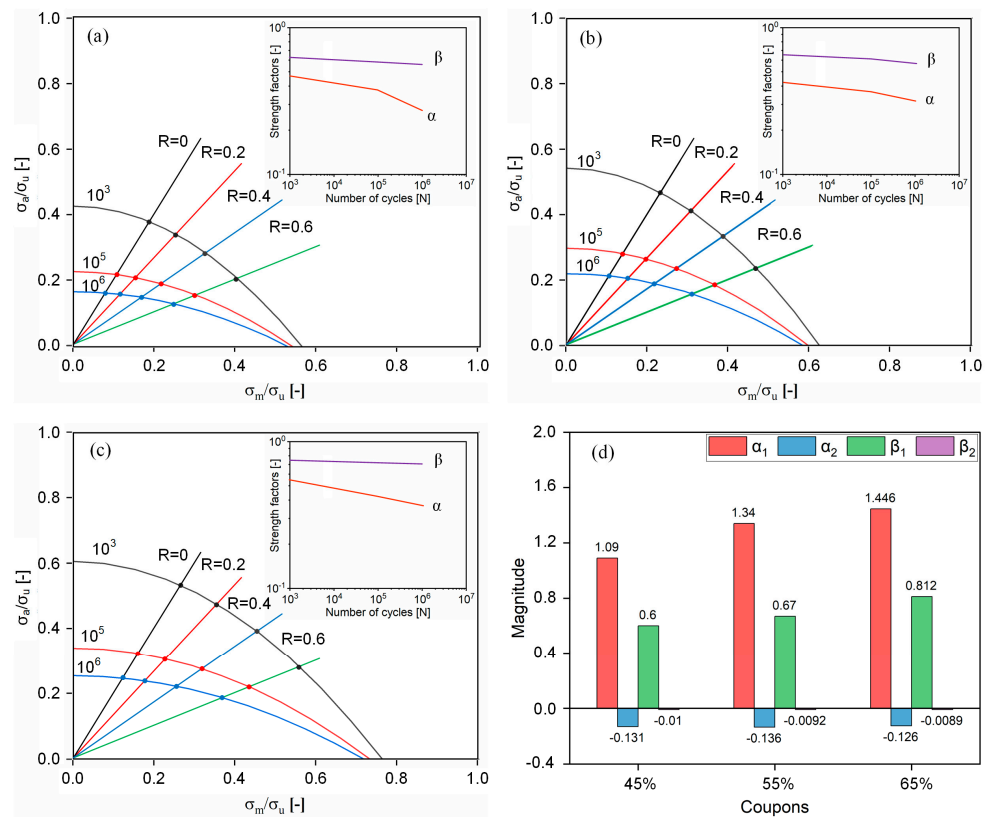


Figure 2. The various fatigue loading directions of the CFRPCs.

### 3. Results and Discussion

#### 3.1. Modified Gerber Equation Parameters

The curves between normalized stress amplitude and normalized mean stress are shown in Figure 3 at various fiber mass fractions. The maximum number of cycles of 106 was considered during the cyclic loading of CFRPCs. As the fiber mass fraction increased, the normalized stress amplitude increased. The ultimate strength of the composites was experimentally determined at different fiber mass fractions. A total of four variations of the stress ratios of 0, 0.2, 0.4, and 0.6 were considered to plot the graph. The Modified Gerber equation was employed to predict fatigue failure once the adjusted  $\alpha$  and  $\beta$  parameters were known, irrespective of orientation and atmospheric conditions. The behavior of  $\alpha$  and  $\beta$  concerning the number of cycles to failure is depicted in the top right of Figures 3–5. It was observed that  $\alpha$  significantly decreased with increased cycles, while  $\beta$  showed minimal changes. For practical applications,  $\alpha$  and  $\beta$  values can be determined for the desired lifetime, enabling the estimation of stress amplitudes ( $\sigma_a$ ) and mean stresses ( $\sigma_m$ ) using the Modified Gerber criteria. The increase in the fiber weight fraction of composites decreased the slope of strength factor  $\alpha$ , while variation in  $\beta$  is found to be negligible. Furthermore, the constants  $\alpha_1$ ,  $\alpha_2$ ,  $\beta_1$ , and  $\beta_2$  of the Modified Gerber equation were determined by the curve fitting at fiber mass fractions of 45%, 55%, and 65%. The percentage decrease in the value of  $\alpha_1$  and  $\alpha_2$  is about 35.6% and 3.81% respectively, when fiber weight percentage is increased from 45% to 65%. There is a negligible increase of 0.08 and 0.1% in the value of  $\beta_1$  and  $\beta_2$ , respectively. Therefore, increasing the fiber mass fraction in the CFRPCs resulted in increased fatigue strength factors, whereas the creep rupture factor has negligible variation.



**Figure 3.** Constant life diagram at fiber mass fraction of (a) 45%, (b) 55%, (c) 65%, and (d) parameters of the Modified Gerber equation.

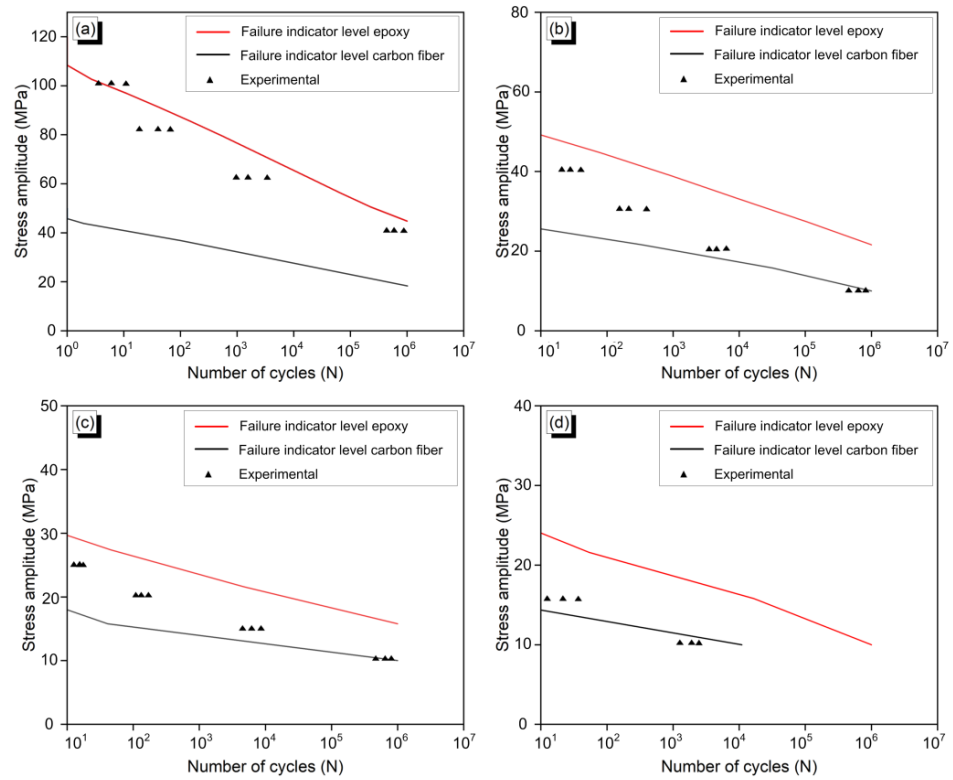


**Figure 4.** Nominal stress amplitude vs. numbers of cycles to failure at loading angle (a) 15° (b) 30° (c) 45°, and (d) 60°, with a stress ratio of 0.2.

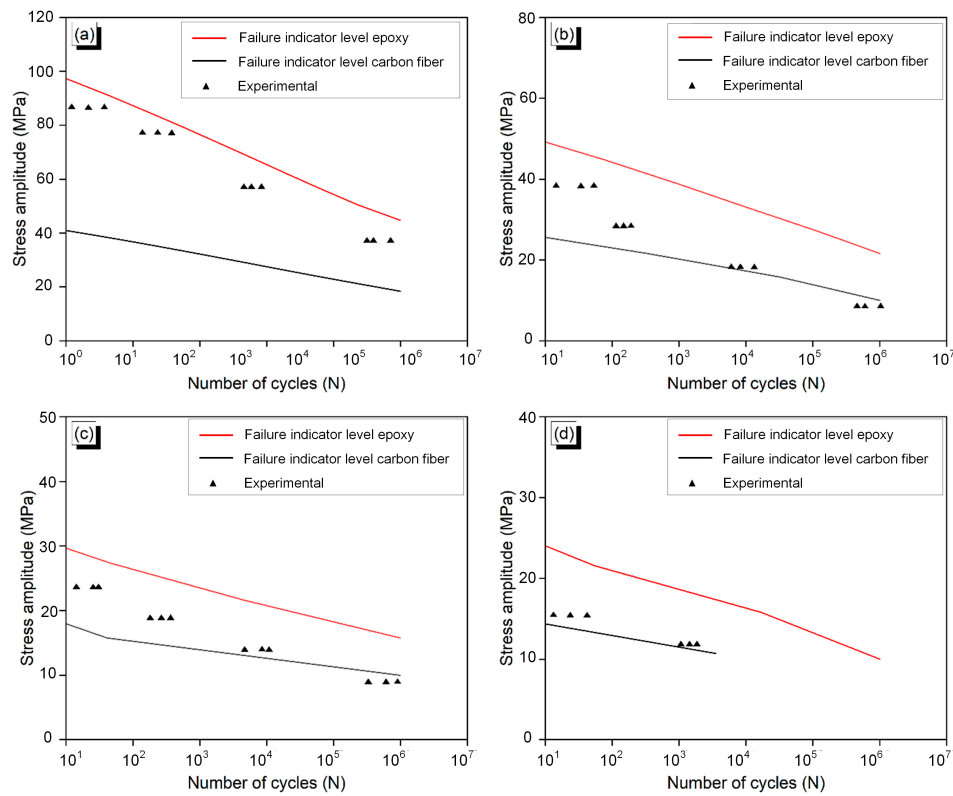


**Figure 5.** Nominal stress amplitude vs. numbers of cycles to failure at loading angle (a) 15° (b) 30° (c) 45°, and (d) 60°, with a stress ratio of 0.4.

### 3.2. Fatigue-Life Prediction

The fatigue-life model for composites under tensile loading has been investigated. S–N curves were obtained at stress ratios of 0.2, 0.4, 0.6, and 0.8 with loading inclinations of 15°, 30°, 45°, and 60°. The number of cycles was obtained at the epoxy and fiber-failure level. At 15° loading inclination, the experimental S–N curve resides near the predicted S–N curve at the epoxy failure indicator level. The experimental results have shown that with an increase in the loading angle, the number of fatigue cycles approaches the predicted S–N curve at the carbon-fiber level.

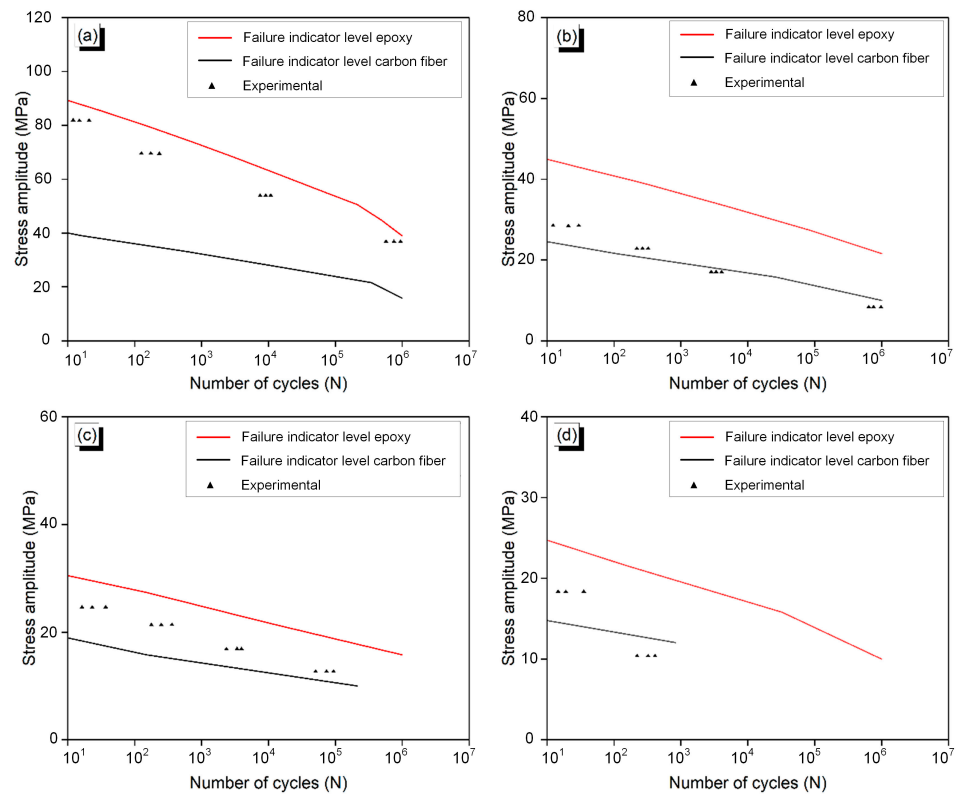
The fatigue analysis reveals interesting findings at a stress ratio of 0.2, demonstrating a notable pattern: the stress amplitude decreases as the load inclination increases, as shown in Figure 4. This suggests a relationship between load inclination and stress distribution. Intriguingly, when comparing these predictions to the experimental results at the same stress ratio, a remarkable similarity emerges, with the experimental data closely following the predicted curve. This alignment strongly indicates that failure occurs at the epoxy level. The failure mechanism at this stress ratio is attributed to matrix failure within the epoxy. The experienced stresses reach a critical threshold, causing the epoxy to deteriorate and ultimately fail. However, it is important to note that as the stress ratio increases beyond 0.2, a significant shift in the failure phenomenon occurs. The failure mode transitions from the epoxy level to the carbon-failure level, suggesting that the carbon material becomes the weak link in the structural integrity, succumbing to the heightened stress conditions. These insights provide valuable information for understanding the failure mechanisms and can aid in optimizing designs to enhance the durability and performance of the materials under different stress ratios.

Figure 5 shows, at 0.4 stress ratio, the maximum stress amplitude lowered down to nearly 100 at 15° load inclination. Experimental results reveal the proximity of the S–N curve with the epoxy-level failure criteria at lower load inclination. At 60° load inclination, the experimental S–N curve coincides with the fiber-failure indicator.

The fiber-failure indicator showed a remarkable resemblance to the experimental results, potentially attributed to the significant difference in extension between carbon fiber and epoxy. This variation in extension might explain why, at a stress ratio of 0.6, the dominance of fiber-related failures prevailed, as shown in Figure 6. The limited extension of carbon fiber, when compared to epoxy, likely contributed to this outcome.

The higher stress-ratio value of 0.8 resulted in composite failure at a low value of stress amplitude, as shown in Figure 7. The higher load inclination resulted in composite failure at a relatively lower stress amplitude and the experimental results are near the carbon-fiber failure indicator curve. At 60° load inclination, fewer than 100 cycles were sustained by the composites before failure. The higher stress ratio (R) means that the minimum stress is closer to the maximum stress in a loading cycle. In other words, the material spends a larger portion of its cycle at higher stress levels. Therefore, the composite failure existed at a much lower amplitude level [27].

In a fiber-reinforced composite material, the von Mises stress is a measure of the equivalent stress that represents the combined effect of normal and shear stresses on the material. The stress distribution in a fiber-reinforced composite depends on the loading direction with respect to the orientation of the fibers. At 0.2 stress ratio, von Mises stress contours are shown in Figure 8. The maximum stress was 254.223 MPa and decreased further with the increase in the loading angle. The decrease in von Mises stress may be attributed to the early failure of the composites. At the loading angle of 60° the von Mises stress reduced to 154.917, which is about a 39% decrease in stress as compared to the stress value at 15° loading.



**Figure 6.** Nominal stress amplitude vs. numbers of cycles to failure at loading angle (a) 15°, (b) 30°, (c) 45°, and (d) 60°, with a stress ratio of 0.6.

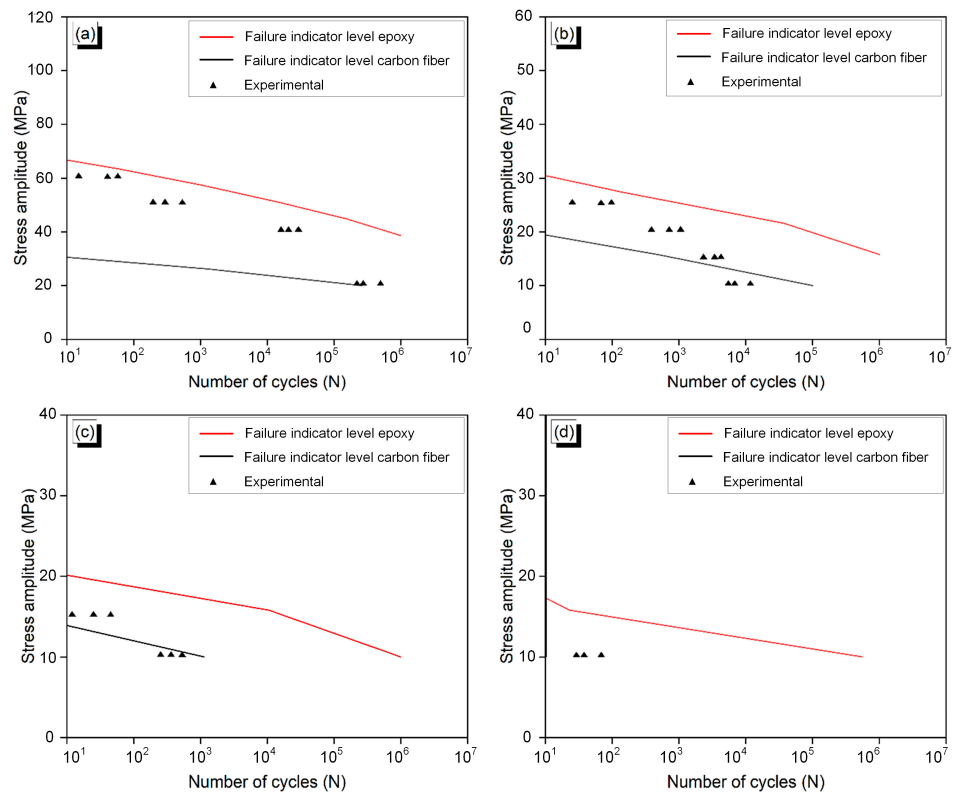


**Figure 7.** Nominal stress amplitude vs. numbers of cycles to failure at loading angle (a) 15°, (b) 30°, (c) 45°, and (d) 60°, with a stress ratio of 0.8.

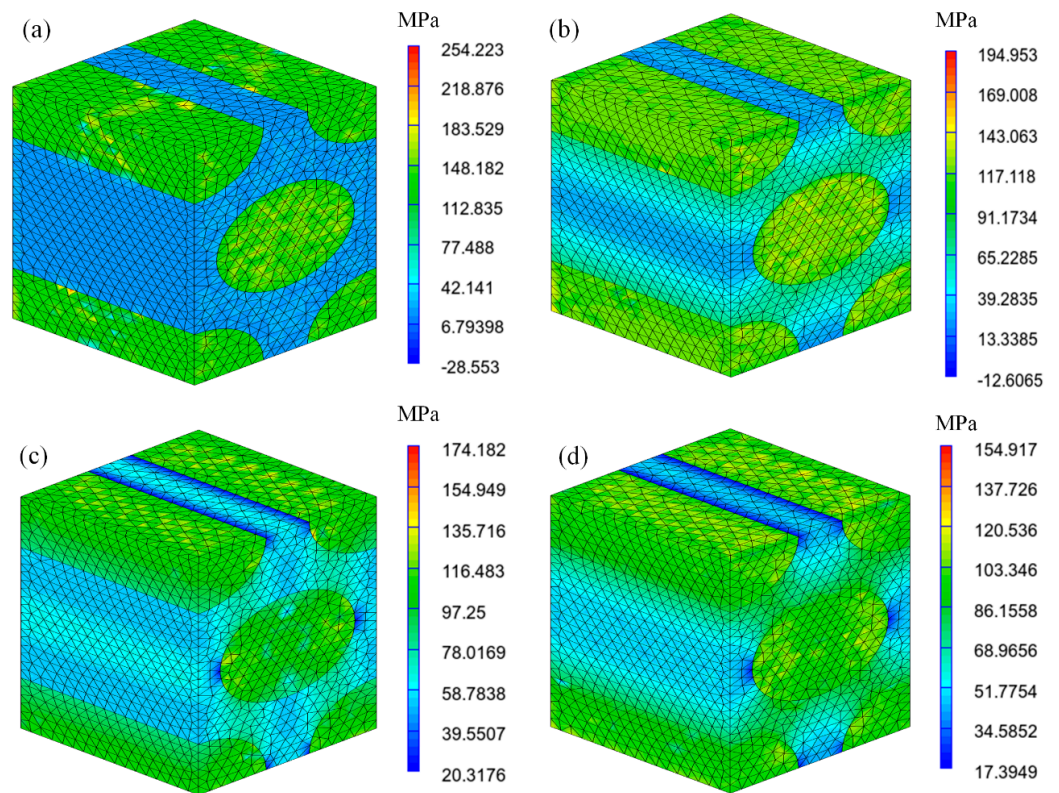


**Figure 8.** Von Mises stress contours at 0.2 stress ratio with load inclinations (a) 15°, (b) 30°, (c) 45°, and (d) 60°.

In Figure 9, the values of von Mises stress at 0.4 stress ratio vary from 237.6 MPa to 140.567 MPa, when the loading angle increases from 15° to 60°. Higher loading inclination dominates the fiber fracture-based failure. When a fiber-reinforced composite is loaded at a lower loading inclination, the fiber properties dominate the stress distribution. The fibers carry most of the applied load, and the matrix primarily provides lateral support. The stress distribution is different when the loading inclination is increased in the fiber-reinforced composite. The fibers are not as effective at carrying the load in this direction, and the matrix bears most of the load [18].

The stress ratio significantly influences the von Mises stress in the composites. The stresses reduce to 220.163 MPa at a 0.6 stress ratio with a 15° loading direction, as shown in Figure 10. At 60° loading direction, the maximum von Mises stress is 127.68 MPa. The matrix binds the fibers together and transfers the loads to the fibers, which carry most of the mechanical stresses at higher loading inclinations.

The stress ratio of 0.8 will result in different von Mises stress levels depending on the loading direction, as shown in Figure 11. The matrix bears more load and the stress level decreases to 198.097 MPa at 15° loading direction. The behavior of fiber-reinforced composites is complex due to their anisotropic nature and the interaction between the fibers and the matrix. The stress ratio will influence how the fibers and matrix share the applied load in different directions, which, in turn, affects the overall von Mises stress distribution in the composite material.

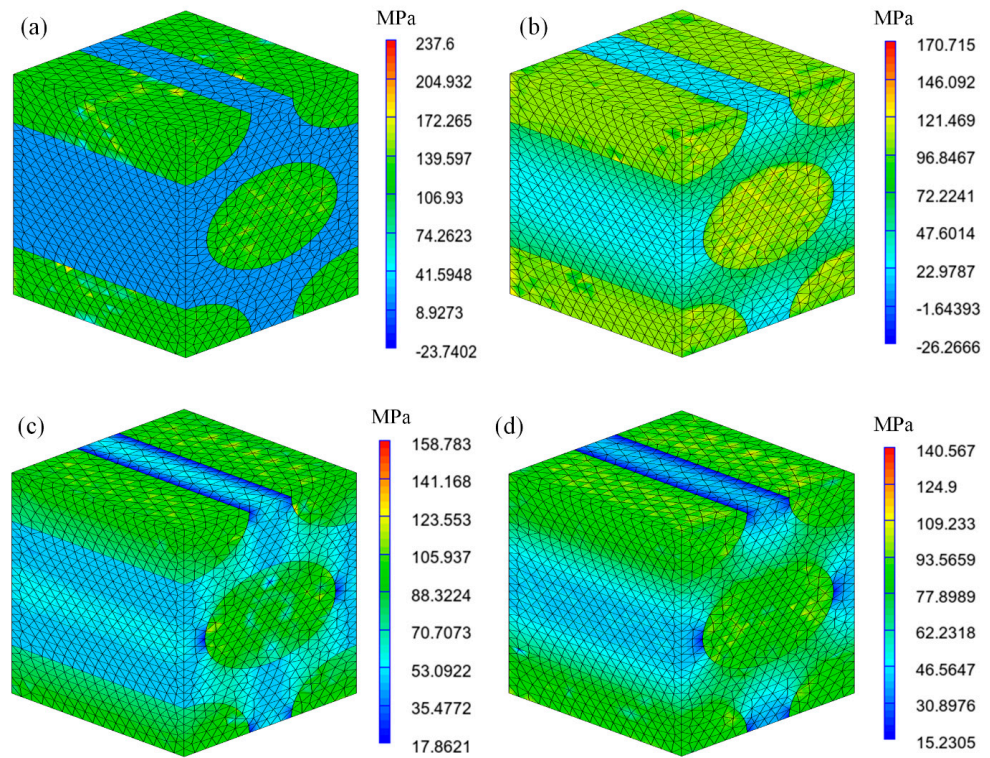


**Figure 9.** Von Mises stress contours at 0.4 stress ratio with load inclinations (a) 15°, (b) 30°, (c) 45°, and (d) 60°.

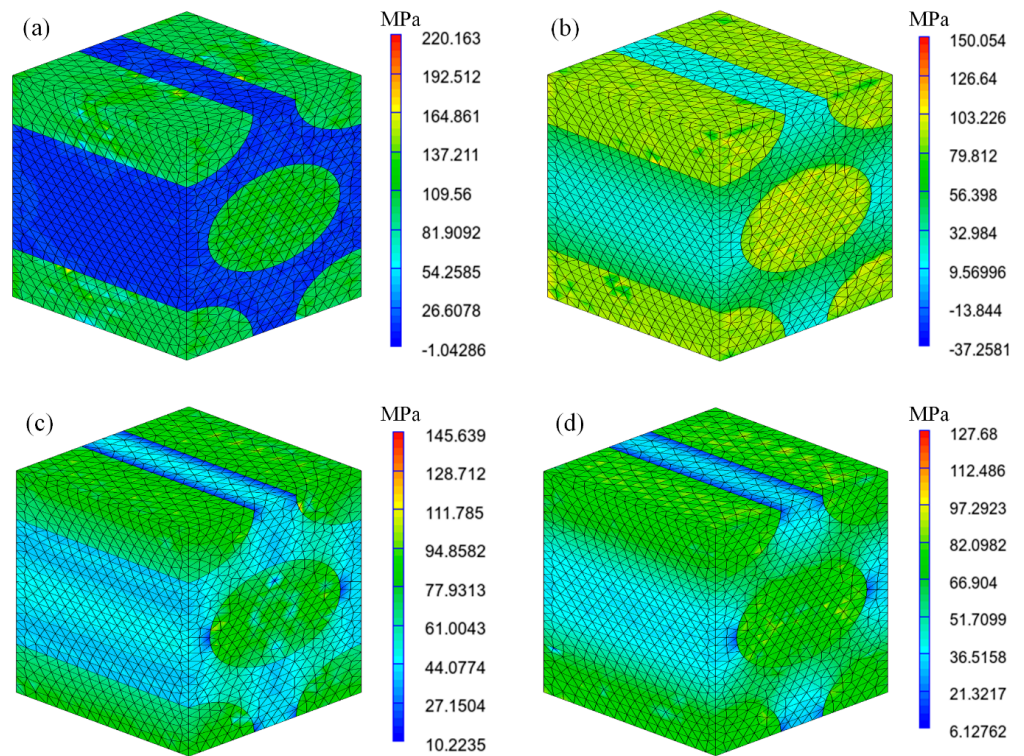


**Figure 10.** Von Mises stress contours at 0.6 stress ratio with load inclinations (a) 15°, (b) 30°, (c) 45°, and (d) 60°.

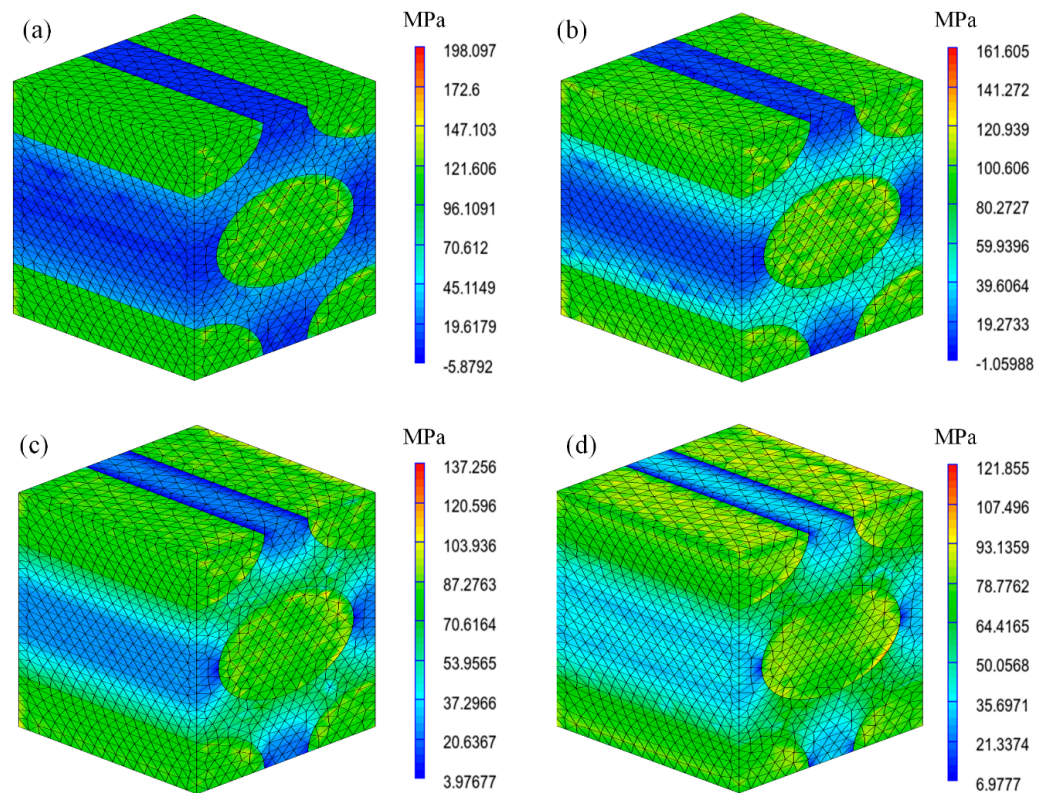


**Figure 11.** Von Mises stress contours at 0.8 stress ratio with load inclinations (a) 15°, (b) 30°, (c) 45°, and (d) 60°.

A further fracture mechanism of the CFRPCs was analyzed by microstructure examination of the fractured composites using scanning electron microscopy, as shown in Figure 12. When a composite material fails due to fatigue, the fracture surfaces of both the fibers and the matrix can provide valuable information about the underlying failure mechanisms and the material's fatigue behavior. Both fiber and matrix fractures were confirmed by microstructural analysis of fractured CFRPCs at various maximum stress levels. Fiber and matrix fracture failure mechanisms vary with the loading direction in fiber-reinforced composites. Lower loading inclination predominantly affects the fiber strength, whereas higher loading inclination affects the matrix strength. When the loading inclination is closer to the direction of the fibers, the fibers bear a greater portion of the applied load. Since fibers are typically stronger and stiffer than the matrix material, a lower loading inclination primarily affects the fiber strength. This means that the behavior of the fibers will influence the composite's overall response more. As the loading inclination moves away from the fiber direction and becomes perpendicular to it, the fibers contribute less to carrying the load. Instead, the matrix material takes on a larger share of the load-bearing responsibility. Since the matrix material is generally weaker and less stiff than the fibers, a higher loading inclination has a greater impact on the matrix strength [34]. The micrograph reveals that the fractured surface in the case of debonding was matrix-dominated, as shown by imprints of fibers on the fractured surface. The clean and sharp lateral fractured surface indicated sudden failure of the fiber at 0.8 stress ratio with 60° loading inclination. The matrix fracture was seen at a lower stress ratio with a lower loading direction.

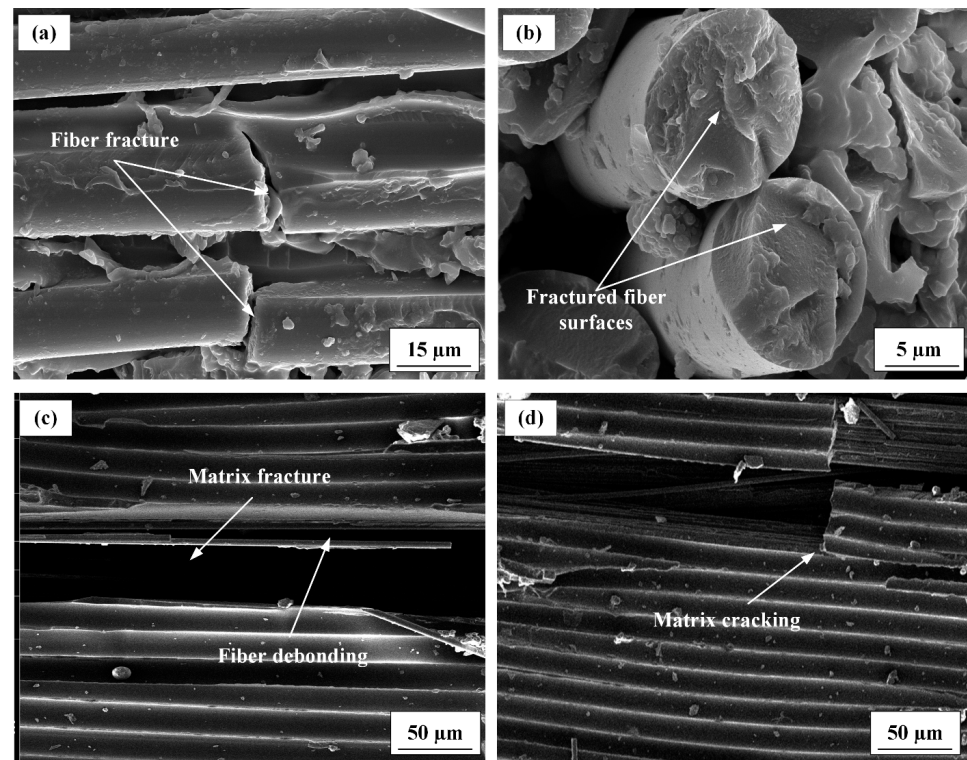


**Figure 12.** SEM images under cyclic loading showing (a) fiber fracture, (b) fiber lateral fractured surface, (c) fiber debonding, and (d) matrix cracking.

#### 4. Conclusions

In conclusion, the integration of meso–macro multiscale analyses and experimentation has proven to be a valuable approach to understanding and predicting the mechanical behavior of fiber composites. By the combination of mesoscale modeling, the details of composites at constituent levels are captured, and a global representation of the material behavior is estimated at the macro scale. Therefore, a more comprehensive understanding of the material response has been achieved by multiscale analyses. The meso–macro analyses approach allows for the incorporation of various failure mechanisms and their interactions at different-length scales. This enables accurate predictions of the material’s fatigue life under different loading conditions. By considering the interaction between fibers and matrix at the meso scale, fatigue modeling provides a deeper understanding of the underlying failure mechanisms and damage initiation and propagation within the composite material. The integration of experimentation plays a crucial role in validating and calibrating the meso–macro models. Experimental testing provides essential data for characterizing the material properties, failure modes, and fatigue behavior. By comparing the model predictions with experimental results, the accuracy and reliability of the models can be assessed, and necessary adjustments can be made to improve their predictive capabilities. The following capabilities of the models are found:

- The model is capable of predicting the fatigue life at the matrix and reinforcement level.
- Fatigue life can be predicted at various stress-ratio levels.
- Fatigue can be predicted in different loading directions.

Overall, the combination of meso–macro multimodeling and experimentation has facilitated significant advancements in our understanding of fiber composite mechanical behavior. The integrated approach has the potential to drive further improvements in material design, optimization of composite structures, and prediction of their performance under various operational conditions. It also offers insights into the development of new composite materials with enhanced mechanical properties and increased durability.

**Author Contributions:** Conceptualization, R.K., S.Z. and H.P.; methodology, R.K.; software, R.K.; validation, R.K.; formal analysis, R.K., S.Z. and H.P.; investigation, R.K.; resources, S.Z., H.P., C.L. and S.-J.H.; data curation, R.K.; writing—original draft preparation, R.K. and M.S.; writing—review and editing, S.Z., H.P., M.S., C.L. and S.-J.H.; visualization, R.K., S.Z., H.P., M.S., C.L. and S.-J.H.; supervision, S.Z., H.P., M.S., C.L. and S.-J.H.; project administration, S.Z., H.P., C.L. and S.-J.H.; funding acquisition, S.-J.H. All authors have read and agreed to the published version of the manuscript.

**Funding:** This research received no external funding.

**Data Availability Statement:** The data presented in this study are available on request from the corresponding author.

**Conflicts of Interest:** The authors declare no conflict of interest.

## References

1. Barile, C.; Casavola, C.; De Cillis, F. Mechanical Comparison of New Composite Materials for Aerospace Applications. *Compos. Part B Eng.* **2019**, *162*, 122–128. [[CrossRef](#)]
2. Verma, N.; Kumar, R.; Zafar, S.; Pathak, H. Vacuum-Assisted Microwave Curing of Epoxy/Carbon Fiber Composite: An Attempt for Defect Reduction in Processing. *Manuf. Lett.* **2020**, *24*, 127–131. [[CrossRef](#)]
3. Holmes, J.; Sommacal, S.; Das, R.; Stachurski, Z.; Compston, P. Characterisation of Off-Axis Tensile Behaviour and Mesoscale Deformation of Woven Carbon-Fibre/PEEK Using Digital Image Correlation and X-Ray Computed Tomography. *Compos. Part B Eng.* **2022**, *229*, 109448. [[CrossRef](#)]
4. Mirzaei, A.H.; Shokrieh, M.M.; Saeedi, A. Fatigue Behavior of Laminated Composites with Embedded SMA Wires. *Compos. Struct.* **2022**, *293*, 115753. [[CrossRef](#)]
5. Alam, P.; Mamalis, D.; Robert, C.; Floreani, C.; Brádaigh, C.M.Ó. The Fatigue of Carbon Fibre Reinforced Plastics—A Review. *Compos. Part B Eng.* **2019**, *166*, 555–579. [[CrossRef](#)]
6. Gamstedt, E.K.; Talreja, R. Fatigue Damage Mechanisms in Unidirectional Carbon-Fibre-Reinforced Plastics. *J. Mater. Sci.* **1999**, *34*, 2535–2546. [[CrossRef](#)]
7. Ansari, M.T.A.; Singh, K.K.; Azam, M.S. Fatigue Damage Analysis of Fiber-Reinforced Polymer Composites—A Review. *J. Reinf. Plast. Compos.* **2018**, *37*, 636–654. [[CrossRef](#)]
8. Arora, G.; Pathak, H. Modeling of Transversely Isotropic Properties of CNT-Polymer Composites Using Meso-Scale FEM Approach. *Compos. Part B Eng.* **2019**, *166*, 588–597. [[CrossRef](#)]
9. Marek, A.; Garbowski, T. Homogenization of Sandwich Panels. *Comput. Assist. Methods Eng. Sci.* **2015**, *22*, 39–50.
10. Buannic, N.; Cartraud, P.; Quesnel, T. Homogenization of Corrugated Core Sandwich Panels. *Compos. Struct.* **2003**, *59*, 299–312. [[CrossRef](#)]
11. Garbowski, T.; Gajewski, T. Determination of Transverse Shear Stiffness of Sandwich Panels with a Corrugated Core by Numerical Homogenization. *Materials* **2021**, *14*, 1976. [[CrossRef](#)] [[PubMed](#)]
12. Staszak, N.; Gajewski, T.; Garbowski, T. Shell-to-Beam Numerical Homogenization of 3D Thin-Walled Perforated Beams. *Materials* **2022**, *15*, 1827. [[CrossRef](#)] [[PubMed](#)]
13. Garbowski, T.; Marek, A. Homogenization of Corrugated Boards through Inverse Analysis. In Proceedings of the OPT-i 2014—1st International Conference on Engineering and Applied Sciences Optimization, Kos Island, Greece, 4–6 June 2014; pp. 1751–1766.
14. Mrówczyński, D.; Knitter-piątkowska, A.; Garbowski, T. Non-Local Sensitivity Analysis and Numerical Homogenization in Optimal Design of Single-Wall Corrugated Board Packaging. *Materials* **2022**, *15*, 720. [[CrossRef](#)] [[PubMed](#)]
15. Vedrtnam, A. Novel Method for Improving Fatigue Behavior of Carbon Fiber Reinforced Epoxy Composite. *Compos. Part B Eng.* **2019**, *157*, 305–321. [[CrossRef](#)]
16. Guo, Y.E.; Shang, D.G.; Cai, D.; Jin, T.; Li, D.H. Fatigue Life Prediction Considering Temperature Effect for Carbon Fibre Reinforced Composites under Variable Amplitude Loading. *Int. J. Fatigue* **2023**, *168*, 107442. [[CrossRef](#)]
17. Vassilopoulos, A.P.; Keller, T. *Modeling the Fatigue Behavior of Fiber-Reinforced Composite Materials Under Constant Amplitude Loading*; Springer: Berlin/Heidelberg, Germany, 2011; ISBN 9781849961813.
18. Brunbauer, J.; Gaier, C.; Pinter, G. Computational Fatigue Life Prediction of Continuously Fibre Reinforced Multiaxial Composites. *Compos. Part B Eng.* **2015**, *80*, 269–277. [[CrossRef](#)]
19. Zhang, W.; Zhou, Z.; Scarpa, F.; Zhao, S. A Fatigue Damage Meso-Model for Fiber-Reinforced Composites with Stress Ratio Effect. *Mater. Des.* **2016**, *107*, 212–220. [[CrossRef](#)]
20. Shokrieh, M.M.; Taheri-Behrooz, F. A Unified Fatigue Life Model Based on Energy Method. *Compos. Struct.* **2006**, *75*, 444–450. [[CrossRef](#)]
21. Huang, Z.; Zhang, W.; Qian, X.; Su, Z.; Pham, D.C.; Sridhar, N. Fatigue Behaviour and Life Prediction of Filament Wound CFRP Pipes Based on Coupon Tests. *Mar. Struct.* **2020**, *72*, 102756. [[CrossRef](#)]
22. Xu, J.; Lomov, S.V.; Verpoest, I.; Daggumati, S.; Van Paepegem, W.; Degrieck, J. A Progressive Damage Model of Textile Composites on Meso-Scale Using Finite Element Method: Fatigue Damage Analysis. *Comput. Struct.* **2015**, *152*, 96–112. [[CrossRef](#)]

23. Kumar, R.; Rani, M.; Zafar, S. Influence of Stacking Sequence on Impact Strength/Hardness of CF/GF Hybrid Composites Fabricated by VARIMC Technique. *Mater. Today Proc.* **2021**, *45*, 4666–4670. [[CrossRef](#)]
24. Li, Y.; Li, N.; Zhou, J.; Cheng, Q. Microwave Curing of Multidirectional Carbon Fiber Reinforced Polymer Composites. *Compos. Struct.* **2019**, *212*, 83–93. [[CrossRef](#)]
25. Kumar, R.; Pathak, H.; Zafar, S. Fracture and Mechanical Behavior of Vacuum-Assisted Microwave Cured Unidirectional Carbon Woven Fabric Reinforced Epoxy Composite. *Proc. Inst. Mech. Eng. Part L J. Mater. Des. Appl.* **2021**, *235*, 400–412. [[CrossRef](#)]
26. Santharam, P.; Marco, Y.; Le Saux, V.; Le Saux, M.; Robert, G.; Raoult, I.; Guévenoux, C.; Taveau, D.; Charrier, P. Fatigue Criteria for Short Fiber-Reinforced Thermoplastic Validated over Various Fiber Orientations, Load Ratios and Environmental Conditions. *Int. J. Fatigue* **2020**, *135*, 105574. [[CrossRef](#)]
27. Mallick, P.K.; Zhou, Y. Effect of Mean Stress on the Stress-Controlled Fatigue of a Short E-Glass Fiber Reinforced Polyamide-6,6. *Int. J. Fatigue* **2004**, *26*, 941–946. [[CrossRef](#)]
28. ASTM D3479-19; Standard Test Method for Tension-Tension Fatigue of Polymer Matrix Composite Materials. ASTM International: West Conshohocken, PA, USA, 2012; Volume 96, p. 6.
29. Su, Y.; Asadi, H.; Nikraz, H. Comparison of Varied Specimen Geometry for Simplified VECD Test with Pulse-Rest Period. *Int. J. Pavement Res. Technol.* **2020**, *13*, 392–401. [[CrossRef](#)]
30. ASTM. Astm D3039/D3039M. *Annu. B. ASTM Stand.* **2014**, 1–13.
31. Ogierman, W.; Kokot, G. Mean Field Homogenization in Multi-Scale Modelling of Composite Materials. *J. Achiev. Mater. Manuf. Eng.* **2013**, *61*, 343–348.
32. Bernasconi, A.; Davoli, P.; Basile, A.; Filippi, A. Effect of Fibre Orientation on the Fatigue Behaviour of a Short Glass Fibre Reinforced Polyamide-6. *Int. J. Fatigue* **2007**, *29*, 199–208. [[CrossRef](#)]
33. De Monte, M.; Moosbrugger, E.; Quaresimin, M. Influence of Temperature and Thickness on the Off-Axis Behaviour of Short Glass Fibre Reinforced Polyamide 6.6—Cyclic Loading. *Compos. Part A Appl. Sci. Manuf.* **2010**, *41*, 1368–1379. [[CrossRef](#)]
34. Zhang, J.; Li, V.C. Effect of Inclination Angle on Fiber Rupture Load in Fiber Reinforced Cementitious Composites. *Compos. Sci. Technol.* **2002**, *62*, 775–781. [[CrossRef](#)]

**Disclaimer/Publisher’s Note:** The statements, opinions and data contained in all publications are solely those of the individual author(s) and contributor(s) and not of MDPI and/or the editor(s). MDPI and/or the editor(s) disclaim responsibility for any injury to people or property resulting from any ideas, methods, instructions or products referred to in the content.